sciendo

DOI 10.2478/ama-2022-0023

acta mechanica et automatica, vol.16 no.3 (2022)

CALCULATION OF THE OPTIMAL BRAKING FORCE DISTRIBUTION IN THREE-AXLE TRAILERS WITH TANDEM SUSPENSION

Zbigniew KAMIŃSKI*

*Faculty of Mechanical Engineering, Bialystok University of Technology, ul. Wiejska 45C, 15-351 Białystok, Poland

z.kaminski@pb.edu.pl

received 8 February 2022, revised 15 March 2022, accepted 16 March 2022

Abstract: Heavy agricultural trailers can be equipped with a three-axle chassis with a tandem axle set at the rear and one mounted on a turntable at the front. In such trailers, selection of the distribution of braking forces that meet the requirements of the EU Directive 2015/68, with regard to braking, largely depends on the type of tandem suspension used. The requirements for brake force distribution in agricultural trailers of categories R3 and R4 are described. On this basis, a methodology for calculating the optimal linear distribution of braking forces, characteristic of agricultural trailers with air braking systems, was developed. An analysis of the forces acting on a 24-tonne three-axle trailer during braking was performed for five different suspensions of the rear tandem axle. An optimization algorithm using the quasi Monte Carlo method was described, on the basis of which a computer program for selection of the linear distribution of braking forces was developed. The calculations were made for an empty and loaded trailer with and without the weight of the tandem suspension. The most uniform distribution of braking forces was obtained for two leaf spring with dynamic equalization and air suspension, in which the ratio of the braking force of the tandem axle and the total braking force varied between 22.9% and 25.5% for the different calculation variants. A large variation in the braking force distribution was achieved for the two leaf spring suspension, in which the ratio of tandem axle braking force and the total braking force ranged from 2.7% to 6.4% for the leading axle and from 27.8% to 36.2% for the trailing axle. The presented calculation methodology can be used in the initial phase of the design of air braking systems for three-axle agricultural trailers.

Key words: agriculture trailer, tandem axle, air braking system, braking force distribution, optimization

1. INTRODUCTION

Heavy agricultural trailers with laden weights of about 25 tonnes can be designed as full three-axle trailers [26]. A full trailer is typically towed via a single-point drawbar that is also used to steer the front axle by rotating the front running gear [7]. At the rear of the trailer is mounted a tandem axle set comprising two axles spaced close to each other, usually from 1.2 m to 1.85 m [8, 13]. Tandem axles are used to increase the load-carrying capacity of a vehicle and to distribute the load between both axles, independent of the road surface roughness [18].

Tandem axle suspension may be grouped according to the basic design [14, 18, 24]. In agricultural trailers, different types of tandem axles are used, that is, walking beam, bogie (with single inverted parabolic spring), two leaf spring, two leaf spring and rods, two leaf spring with dynamic equalization and air suspension [1, 3, 29, 30].

In many types of tandem suspension for agricultural trailers, the axle load is transferred through the load leveller or equalizer beam used to balance the axle loads during normal operation with the brakes not applied [25]. Unfortunately, some mechanisms that are used to create good static load equalization have just the opposite effect on the dynamic load transfer [13]. When braking in vehicles with two leaf spring tandem suspension (two leaf spring and rods), the sum of the front spring seat force is less than the sum of the rear seat force, and the corresponding leading and trailing axle loads are no longer equal [25]. This resulting action is called the inter-axle load transfer [13, 25]. Transferring the load between the axles causes the front axle to lock before the rear axle is locked and has a negative effect on braking performance. For example, in a truck equipped with two-elliptic leaf suspension the dynamic load of the leading axle approaches zero for a deceleration of approximately 0.55 g [18]. The friction utilization diagram indicates that the tandem rear axle is slightly braked while the front axle is greatly underbraked. If lockup occurs on the leading axle, then the directional stability is reduced. An additional improvement can be achieved by changing the tandem axle design to include push rods. Then, the wheels unlocked deceleration increases to 0.38 g from an original value of 0.25 g for an adhesion coefficient of 0.6 [18]. The directional stability can be completely lost if lockup occurs on the trailing axle [13]. Another unwanted result of poor inter-axle load transfer is that the suspension can produce an under-damped mode. Occasionally, this can result in a 'tandem hoop', which can cause a partial degradation of the vehicle's braking and handling performance [13]. The survey results [11] showed that the semi-trailer with the air suspension system can reduce the dynamic load coefficient from 14.8% to 29.3%, in comparison with the semi-trailer using the leaf spring suspension system.

Since 2016, EU agricultural vehicle legislation [6] has required agricultural trailers to achieve the same braking performance as commercial vehicle trailers (min. 50% braking efficiency for vehicles operating above 30 km/h). In addition, for agricultural trailers with a total mass of more than 3,500 kg (categories R3 and R4) and moving at a speed of more than 40 km/h, a specific distribu-

tion of braking forces between the axles of the vehicle is required. The braking efficiency has a direct influence on the vehicle braking distance and the vehicle's travelling direction stability in any road condition [28]. The adoption of the new European legislation in the field of agricultural vehicles places a high demand on the manufacturers of agricultural trailers, tractors and machinery in terms of braking systems [9].

The design process of a new brake system begins with the selection of the brake force distribution [21]. Generally, for the correct design of a vehicular brake system, it is essential that the ideal brake force distribution among the individual axles be known for empty and loaded vehicles [19]. In the case of two-axle vehicles, the relationships are simple and can be given in terms of either the vehicle deceleration or the rear axle brake force as a function of the front axle brake force [10]. Advanced optimization methods and strategies for selecting the distribution of braking forces are constantly being developed for passenger cars [10, 27, 34] and trucks [28, 35].

An analytical method of calculation of the brake force distribution in two-axle agricultural trailers was described in [16 and 20]. For a three-axle trailer, however, the analysis is more complex as the middle and rear axle loads are functions of the loading as well as the type and the geometry of the tandem axle suspension [18]. Therefore, even for three-axle vehicles with the simplest tandem suspensions, like walking beam and bogie [16] or two-elliptic leaf spring suspension [28], optimization methods are used to calculate and select the braking force distribution.

This paper is the result of a demand by agricultural machinery companies for new solutions for the calculation of the braking force distribution in three-axle trailers with different types of tandem suspension, filling a gap in the research. The quasi Monte Carlo method was used to search for an optimal linear force distribution, which is mostly used in the air brake system of trailers.

The rest of the paper is organized as follows: in section 2, the requirements of the braking force distribution of three-axle trailers are described; in section 3, the analysis of forces acting during braking on a three-axle trailer with different types of tandem suspension is presented; in section 4, the quasi Monte Carlo method and the algorithm of linear brake force distribution are described. The results of the optimization calculation for the different tandem axles are analysed and discussed in section 5. Finally, the summary and conclusions are drawn in section 6.

The results of the paper are expected to provide a reference for designing and evaluating the braking system of three-axle agricultural trailers and improving their braking performance.

2. REQUIREMENTS FOR BRAKING PERFORMANCE AND BRAKE FORCE DISTRIBUTION FOR THREE-AXLE TRAILER

When choosing the distribution of braking force between vehicle axles, an ideal distribution should be sought. The ideal braking condition is achieved when each axle and each axle assembly has the same rate of utilized adhesion, which is equal to the braking rate z of the vehicle. For a three-axle trailer with tandem axle at the rear, this condition can be written as follows:

$$f_1 = f_2 = f_{2i} = z \qquad z = \frac{T_1 + \sum T_{2i}}{R_1 + \sum R_{2i}} \tag{1}$$

where T_1, and R_1 are the braking force and normal reactions of the road surface on the wheels of the front axle, T_{2i} and R_{2i} are the braking forces and normal reactions of the road surface on the wheels of the rear tandem axle, and i is the axle number in the rear axle assembly.

The adhesion utilization rates used by the front axle and rear axle assembly are calculated based on the following relationship:

$$f_1 = \frac{T_1}{R_1} \qquad f_2 = \frac{\sum f_{2i} R_{2i}}{\sum R_{2i}} \tag{2}$$

With the braking distribution at the ideal level, the straight line stopping distance is minimized as a result of each axle reaching its maximum braking force capability [23], and the braking efficiency requirements are met with reserve (Tab. 1).

Tab. 1. The required service braking efficiency for towed agricultural vehicles [6]

Vehicle category	Braking rate z [%] at p = 6.5 bar	
	v≤30 km/h	v>30 km/h
Trailers R2, R3, R4 and towed machines S2	≥35%	≥50%

Due to trailer load variations, it is practically impossible to achieve an ideal brake distribution, even when using braking force regulators. Therefore, for agricultural vehicles with speed above 40 km/h, the allowable limits for derogation of the adhesion utilization rates for individual axles against the ideal distribution have been determined. In the considerations regarding the distribution of brake forces, each part of a tractor-trailer unit is treated as a single vehicle, without taking into account the force in the coupling. From 2016, two solutions have been allowed, as shown in Fig. 1 [6].

The first solution: the adhesion utilization rate for each axle assembly must meet the condition of ensuring the minimum required braking performance as:

$$f_{1,2} \le \frac{z+0.07}{0.85} \quad \text{when} \quad 0.1 \le z \le 0.61 \tag{3}$$

and the condition of previous locking of the front axle wheels to ensure directional stability as:

$$f_1 > z > f_2 \quad \text{when} \quad 0.15 \le z \le 0.30 \tag{4}$$

The second solution: the adhesion utilization rates by the axles should be within a given band, and then the limits of wheel locking are determined by the following relationships:

$$\begin{matrix} f_1 \ge z - 0.08 \\ f_{1,2} \le z + 0.08 \end{matrix} \quad \text{when} \quad 0.15 \le z \le 0.30 \tag{5}$$

In addition, the adhesion utilization curve for the rear axle assembly should fulfill the condition:

$$f_2 \le \frac{z-0.02}{0.74} \quad \text{when} \quad 0.30 \le z \le 0.61 \tag{6}$$

For precise calculations, the divisor in the inequality (6) should be set as 0.7381.

DOI 10.2478/ama-2022-0023

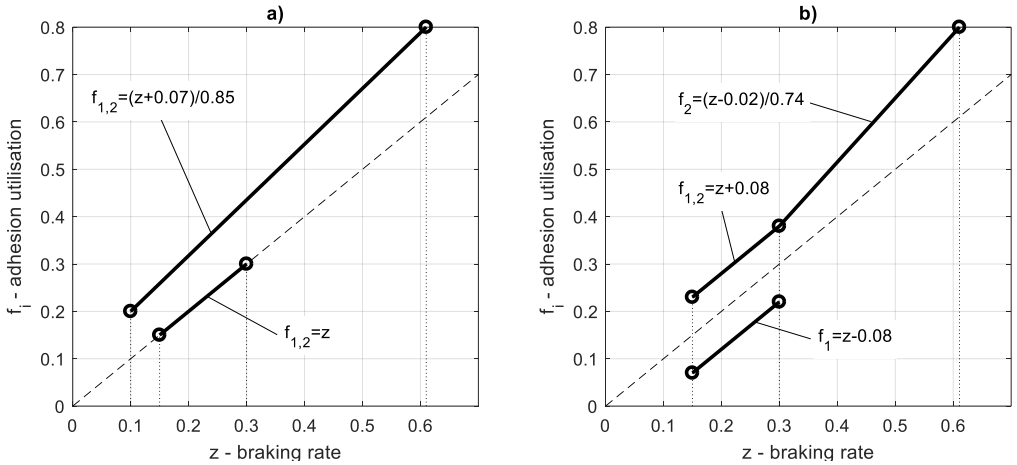

Fig. 1. Limit values of adhesion utilization in accordance with the Commission Delegated Regulation (EU) 2015/68 [6]: (a) – first solution, (b) – second solution

The wheel-lock sequence requirements are regarded as met if the adhesion utilized by the front axle is greater than that utilized by at least one of the rear axles at braking rates between 0.15 and 0.30 [6]:

$$f_1 > f_{2i} \quad \text{for any } i \tag{7}$$

3. BRAKING OF THREE-AXLE TRAILER

For analysis of the brake force distribution, a rigid two-dimensional trailer model is proposed. In this model a suspension system with a different type and geometry of tandem axle is used. The forces acting on a decelerating three-axle agricultural trailer with tandem suspension are illustrated in Fig. 2. For simplicity, it is assumed that aerodynamic and rolling resistances are omitted.

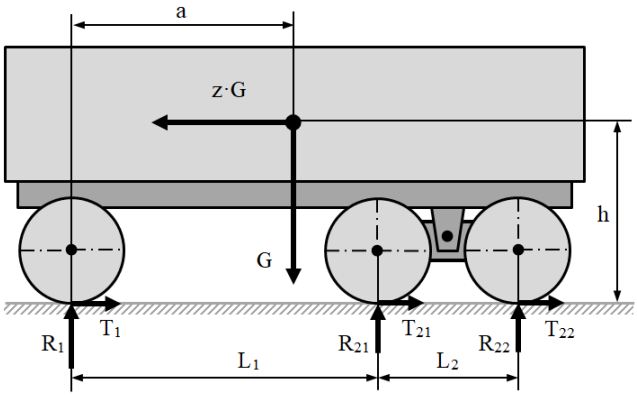

Fig. 2. Forces acting on a three-axle trailer with tandem suspension (ISO coordinate system [15])

The forces T_1, T_{21} and T_{22} which induce braking deceleration are obtained from the axle brake force and are considered to be known functions of the brake line pressure [4, 6]. Using the notation from Fig. 2, the equations of force and moment equilibrium are given as:

$$\sum X = z \cdot G - T_1 - T_{21} - T_{22} = 0 \tag{8}$$

$$\sum Z = R_1 + R_{21} + R_{22} - G = 0 \tag{9}$$

$$\sum M_1 = R_{21}L_1 + R_{22}(L_1 + L_2) - G \cdot a + z \cdot G \cdot h = 0 \tag{10}$$

where T_1, T_{21} and T_{22} are the brake forces, R_1, R_{21} and R_{22} are the axle loads, L_1 is the inter-axle spacing, L_2 is the tandem axle spread, a is the distance from the centre of gravity to the front axle, h is the centre of gravity height, G is the trailer weight and z is the braking rate.

To determine the vertical reactions, the system of Eqs. (8)–(10) should be supplemented with an additional relationship between reactions R_{21} and R_{22}, which depends on the type and parameters of the tandem axle suspension.

3.1. Walking beam and bogie suspension

The simplest form of tandem axle suspension is a walking beam [1] located on either side of the vehicle (Fig. 3a). The walking beams are pivotally mounted onto the hanger of the trailer frame at a location intermediate between the forward and rear axles. The tandem axles may be rigidly attached to the ends of the walking beam using, for example, a U-bolt. In the bogie suspension, instead of walking beams, parabolic tapered springs are mounted upside down to the frame (Fig. 3b). The springs are anchored to the trailer frame by a cradle and U-bolts to allow for motion between the two axles [3].

The forces acting on the walking beam and bogie suspension are shown in Fig. 3.

Both tandem suspensions can be described by the same set of force and moment equilibrium equations as:

$$\sum X = z \cdot G_2 - T_{21} - T_{22} + T_2 = 0 \tag{11}$$

$$\sum Z = R_{21} + R_{22} - R_2 - G_2 = 0 \tag{12}$$

$$\sum M_2 = R_{22}d_2 - R_{21}d_1 + G_2 b_2 - z \cdot G_2(h_s - h_2) + (T_{21} + T_{22})h_s = 0 \tag{13}$$

where T_2 and R_2 are the horizontal and vertical reaction forces in the single-point support between the suspension and trailer frame, d_1 and d_2 are the beam (parabolic spring) lengths, h_s is the height of the support position, b_2 is the distance of the centre of unsprung weight from a support, h_2 is the height of the centre of unsprung weight and G_2 is the unsprung weight.

DOI 10.2478/ama-2022-0023

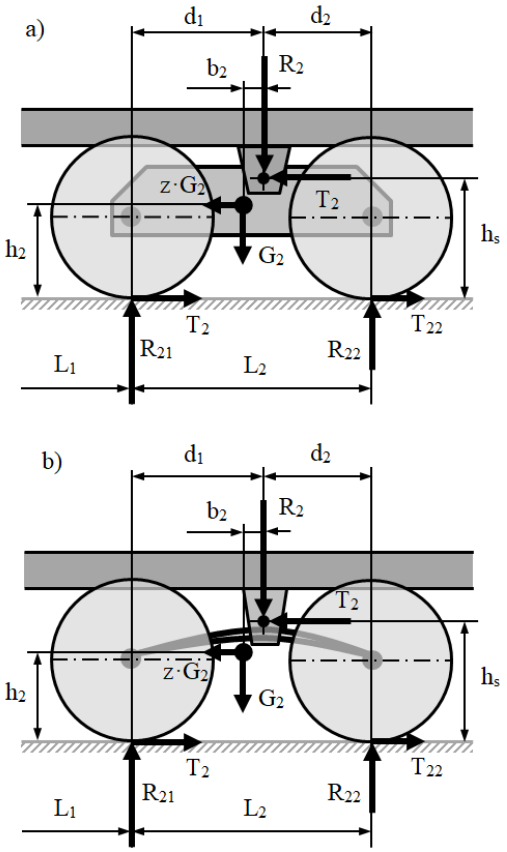

Fig. 3. Forces acting on a (a) walking beam and (b) bogie suspension

By solving the system of Eqs. (9), (10) and (13) together, taking into account from Eq. (8) that $T_{21} + T_{22} = z \cdot G - T_1$, the dynamic axle loads during braking on a three-axle trailer are obtained as:

$$R_1 = G\left(1 - \frac{a}{L} + z\frac{h}{L}\right) - G_2\left(\frac{b_2}{L} - z\frac{h_s - h_2}{L}\right) - (z \cdot G - T_1)\frac{h_s}{L} \tag{14}$$

$$R_{21} = G\left(\frac{a}{L} - z\frac{h}{L}\right)\frac{d_2}{L_2} + \frac{L_1 + L_2}{L_2}\left[G_2\left(\frac{b_2}{L} - z\frac{h_s - h_2}{L}\right) + (z \cdot G - T_1)\frac{h_s}{L}\right] \tag{15}$$

$$R_{22} = G\left(\frac{a}{L} - z\frac{h}{L}\right)\frac{d_1}{L_2} - \frac{L_1}{L_2}\left[G_2\left(\frac{b_2}{L} - z\frac{h_s - h_2}{L}\right) + (z \cdot G - T_1)\frac{h_s}{L}\right] \tag{16}$$

where $L_2 = d_1 + d_2$ is the tandem wheelbase and $L = L_1 + d_1$ is the trailer wheelbase.

By omitting the unsprung weight G2, Eqs. (14)–(16) can be simplified and presented in a slightly different form [16].

3.2. Two leaf spring suspension

In two leaf spring tandem suspension, the two types of springs most commonly available are the double eye leaf spring and the slipper spring. In agricultural trailers the second type is more popular [1, 3, 29]. Slipper springs have an eye formed at one end only, with the other end formed into a reverse curve. The front eye of the leading and trailing spring is pivotally attached directly to the front hanger and equalizer beam, respectively, with pin joints (Fig. 4). The rear end of the springs is captured in the equalizer beam or rear hanger.

The forces acting on the two leaf spring suspension with two unsprung weights are shown in Fig. 4.

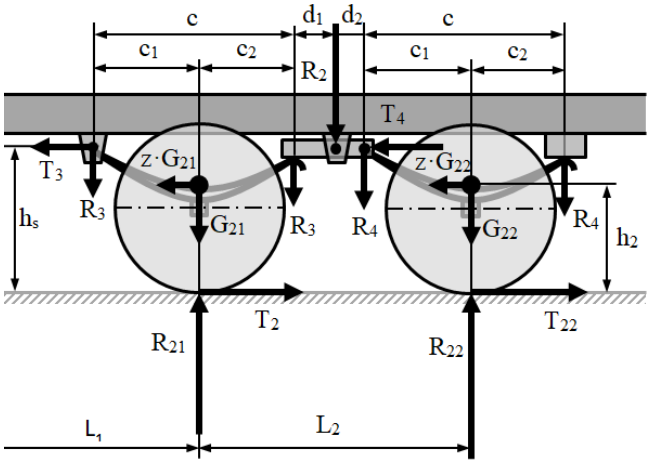

Fig. 4. Forces acting on a two leaf spring suspension

For the unsprung weight G_{21}, the following force and moment equilibrium equations are applicable:

$$\sum X = z \cdot G_{21} - T_{21} + T_3 = 0 \tag{17}$$

$$\sum Z = R_{21} - R_3 - R_{32} - G_{21} = 0 \tag{18}$$

$$\sum M_3 = -R_{32}c + R_{21}c_1 - G_{21}c_1 - z \cdot G_{21}(h_s - h_2) + T_{21}h_s = 0 \tag{19}$$

The equations of force and moment equilibrium for the unsprung weight of the G_{22} suspension are written as:

$$\sum X = z \cdot G_{22} - T_{22} + T_4 = 0 \tag{20}$$

$$\sum Z = R_{22} - R_4 - R_{42} - G_{22} = 0 \tag{21}$$

$$\sum M_4 = R_{42}c - R_{22}c_2 + G_{22}c_2 - z \cdot G_{22}(h_s - h_2) + T_{22}h_s = 0 \tag{22}$$

From Eqs. (19) and (22), the reactions acting on the ends of the equalizer beam are determined as:

$$R_{32} = (R_{21} - G_{21})\frac{c_1}{c} - z \cdot G_{21}\frac{h_s - h_2}{c} + T_{21}\frac{h_s}{c} \tag{23}$$

$$R_{32} = [(R_{21} - G_{21})c_1 - z \cdot G_{21}(h_s - h_2) + T_{21}h_s]/c$$

$$R_{42} = (R_{22} - G_{22})\frac{c_2}{c} + z \cdot G_{22}\frac{h_s - h_2}{c} - T_{22}\frac{h_s}{c} \tag{24}$$

$$R_{42} = [(R_{22} - G_{22})c_2 + z \cdot G_{22}(h_s - h_2) - T_{22}h_s]/c$$

After substituting the expressions (23) and (24) into the equilibrium equation of force moments acting on the equalizer beam:

$$R_{32}d_1 = R_{42}d_2 \tag{25}$$

A new relationship is obtained which, together with Eqs. (9) and (10), creates a system of three equations enabling the determination of the dynamic axle loads during braking of the trailer:

$$R_1 = G - \frac{L_2}{MN}\left\{G(a - z \cdot h)\frac{c_1(d_1 - d_2) + c \cdot d_2}{L_2} + G_{21}d_1[c_1 + z(h_s - h_2)] - G_{22}d_2[c_2 - z(h_s - h_2)] - (T_{21}d_1 + T_{22}d_2)h_s\right\} \tag{26}$$

$$R_{21} = \frac{L_1+L_2}{MN}\Big\{G(a - z\cdot h)\frac{d_2c_2}{L_1+L_2} + G_{21}d_1[c_1 + z(h_s - h_2)] - G_{22}d_2[c_2 - z(h_s - h_2)] - (T_{21}d_1 + T_{22}d_2)h_s\Big\} \quad (27)$$

$$R_{22} = \frac{L_1}{MN}\Big\{G(a - z\cdot h)\frac{c_1d_1}{L_1} - G_{21}d_1[c_1 + z(h_s - h_2)] + G_{22}d_2[c_2 - z(h_s - h_2)] + (T_{21}d_1 + T_{22}d_2)h_s\Big\} \quad (28)$$

where $MN = c_2d_2L_1 + c_1d_1(L_1 + L_2)$

3.3. Two leaf–two rod suspension

A different version of the tandem axle configuration uses two springs with slipper-type ends only. Vertical forces are transmitted into the trailer frame by the front and rear hanger brackets and pivoted equalizer beam [1, 3, 29]. Longitudinal forces are transmitted by connecting the radius rods between the axles and front and centre hanger bracket, respectively (Fig. 5).

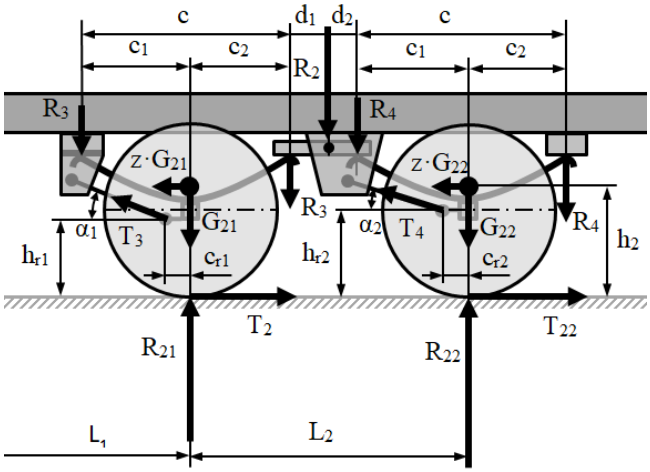

Fig. 5. Forces acting on a two leaf-two rod suspension

The parameters α_1 and α_2 as well as h_{r1} and h_{r2} have a significant impact on the suspension's operation. This design uses a decreased radius rod angle α_2 and a reduction in pivot height h_{r2} at the rear axle to reduce inter-axle load transfer during braking [25].

The following force and moment equilibrium equations for unsprung weights G_{21} and G_{22} are applicable:

$$\sum X = z\cdot G_{21} - T_{21} + T_3\cos\alpha_1 = 0 \quad (29)$$

$$\sum Z = R_{21} + T_3\sin\alpha_1 - R_3 - R_{32} - G_{21} = 0 \quad (30)$$

$$\sum M_3 = -R_{32}c + R_{21}c_1 - G_{21}c_1 - z\cdot G_{21}(h_s - h_2) + T_{21}h_s - T_3\cos\alpha_1\,(h_s - h_{r1}) + T_3\sin\alpha_1\,(c_1 - c_{r1}) \quad (31)$$

$$\sum X = z\cdot G_{22} - T_{22} + T_4\cos\alpha_2 = 0 \quad (32)$$

$$\sum Y = R_{22} + T_4\sin\alpha_2 - R_4 - R_{42} - G_{22} = 0 \quad (33)$$

$$\sum M_4 = R_{42}c - R_{22}c_2 + G_{22}c_2 - z\cdot G_{22}(h_s - h_2) + T_{22}h_s - T_4\cos\alpha_2\,(h_s - h_{r2}) - T_4\sin\alpha_2\,(c_2 + c_{r2}) \quad (34)$$

From Eqs. (31) and (34), the reaction forces acting on the ends of the equalising beam are determined as:

$$R_{32} = (R_{21} - G_{21})\frac{c_1}{c} - z\cdot G_{21}\frac{h_{r1}-h_2}{c} + T_{21}\frac{h_{r1}}{c} + (T_{21} - z\cdot G_{21})\tan\alpha_1\frac{c_1-c_{r1}}{c} \quad (35)$$

$$R_{42} = (R_{22} - G_{22})\frac{c_2}{c} + z\cdot G_{22}\frac{h_{r2}-h_2}{c} - T_{22}\frac{h_{r2}}{c} + (T_{22} - z\cdot G_{22})\tan\alpha_2\frac{c_2+c_{r2}}{c} \quad (36)$$

which are interrelated by the equation of moments of forces:

$$R_{32}d_1 = R_{42}d_2 \quad (37)$$

Solving Eqs. (9), (10) and (35)–(37) together, the trailer axle loads are obtained as:

$$R_1 = G - \frac{L_2}{MN}\Big\{G(a - z\cdot h)\frac{c_1(d_1-d_2)+c\cdot d_2}{L_2} + G_{21}d_1[c_1 + z(h_{r1} - h_2)] - G_{22}d_2[c_2 - z(h_{r2} - h_2)] - (T_{21}d_1h_{r1} + T_{22}d_2h_{r2}) + ED\Big\} \quad (38)$$

$$R_{21} = \frac{L_1+L_2}{MN}\Big\{G(a - z\cdot h)\frac{d_2(c-c_1)}{L_1+L_2} + G_{21}d_1[c_1 + z(h_{r1} - h_2)] - G_{22}d_2[c_2 - z(h_{r2} - h_2)] - (T_{21}d_1h_{r1} + T_{22}d_2h_{r2}) + ED\Big\} \quad (39)$$

$$R_{22} = \frac{L_1}{MN}\Big\{G(a - z\cdot h)\frac{c_1d_1}{L_1} - G_{21}d_1[c_1 + z(h_{r1} - h_2)] + G_{22}d_2[c_2 - z(h_{r2} - h_2)] + (T_{21}d_1h_{r1} + T_{22}d_2h_{r2}) - ED\Big\} \quad (40)$$

where: $MN = d_2L_1c_2 + c_1d_1(L_1 + L_2)$

$$ED = (T_{22} - z\cdot G_{22})\tan\alpha_2\,d_2(c_2 + c_{r2}) - (T_{21} - z\cdot G_{21})\tan\alpha_1d_1\,(c_1 - c_{r1})$$

Eqs. (38)–(40) simplify significantly if $\alpha_1 = \alpha_2 = 0$, because then ED = 0.

3.4. Two leaf spring with equalization

A tandem two leaf spring suspension with equalization [18] has two slipper springs and mechanical braking load compensation (Fig. 6). The rear end of the front spring is connected to the rear end of the rear spring by a rocker arm pivotally connected to a centre hanger bracket. This rocker arm ensures that static (and impact) loads are equally distributed between the two axles. Another design solution for a non-reactive tandem suspension with a bell crank lever and rod linkage is described in [14]. The forces acting on the two leaf spring suspension with equalization are shown in Fig. 6.

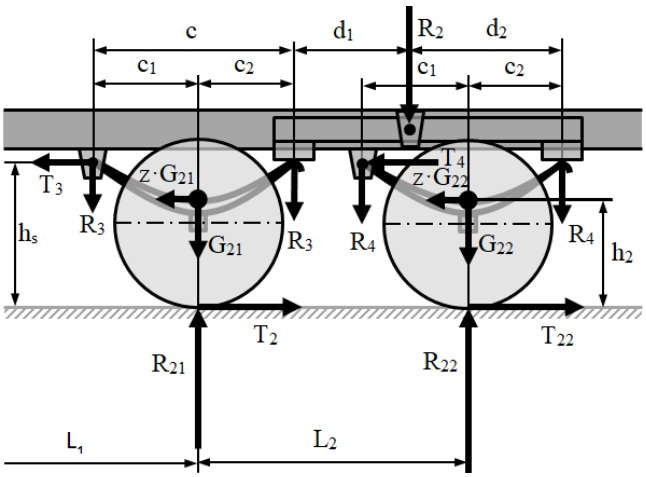

Fig. 6. Forces acting on two leaf spring suspension with equalization

DOI 10.2478/ama-2022-0023

The equations of force and moment equilibrium for the unsprung weights G_{21} and G_{22} of suspension are written as:

$$\sum X = z \cdot G_{21} - T_{21} + T_3 = 0 \quad (41)$$

$$\sum Z = R_{21} - R_3 - R_{43} - G_{21} = 0 \quad (42)$$

$$\sum M_3 = -R_{43}c + R_{21}c_1 - G_{21}c_1 - z \cdot G_{21}(h_s - h_2) + T_{21}h_s = 0 \quad (43)$$

$$\sum X = z \cdot G_{22} - T_{22} + T_2 = 0 \quad (44)$$

$$\sum Z = R_{22} - R_2 - R_{42} - G_{22} = 0 \quad (45)$$

$$\sum M_4 = -R_{42}c + R_{22}c_1 - G_{22}c_1 - z \cdot G_{22}(h_s - h_2) + T_{22}h_s = 0 \quad (46)$$

From Eqs. (43) and (47), the reaction forces acting on the ends of the equalizing beam are calculated as:

$$R_{43} = (R_{21} - G_{21})\frac{c_1}{c} - z \cdot G_{21}\frac{h_s - h_2}{c} + T_{21}\frac{h_s}{c} \quad (47)$$

$$R_{42} = (R_{22} - G_{22})\frac{c_1}{c} - z \cdot G_{22}\frac{h_s - h_2}{c} + T_{22}\frac{h_s}{c} \quad (48)$$

which are related by the equilibrium of moments equation:

$$R_{43}d_1 = R_{42}d_2 \quad (49)$$

By solving the system of Eqs. (9), (10), (47)–(49), the dynamic axle loads are obtained during braking the trailer as:

$$R_1 = \frac{1}{L}\left[G(L - a + z \cdot h) - (G_{21}d_1 - G_{22}d_2)\left(1 + z\frac{h_s - h_2}{c_1}\right) + (T_{21}d_1 - T_{22}d_2)\frac{h_s}{c_1}\right] \quad (50)$$

$$R_{21} = \frac{1}{L}\left[G(a - z \cdot h)\frac{d_2}{L_2} + (G_{21}d_1 - G_{22}d_2)\frac{L_1 + L_2}{L_2}\left(1 + z\frac{h_s - h_2}{c_1}\right) - \frac{L_1 + L_2}{L_2}(T_{21}d_1 - T_{22}d_2)\frac{h_s}{c_1}\right] \quad (51)$$

$$R_{22} = \frac{1}{L}\left[G(a - z \cdot h)\frac{d_1}{L_2} - (G_{21}d_1 - G_{22}d_2)\frac{L_1}{L_2}\left(1 + z\frac{h_s - h_2}{c_1}\right) + \frac{L_1}{L_2}(T_{21}d_1 - T_{22}d_2)\frac{h_s}{c_1}\right] \quad (52)$$

where $L_2 = d_1 + d_2$ and $L = L_1 + d_1$

3.5. Air suspension

In the air suspension the air springs are mounted onto the trailing arms via a cross-member and attached to the frame on the top (Fig. 7). The trailing arms mount pivotally to the hanger brackets and axle housings. All the air bags are connected with one another through air pipes to balance the axle loads. The vertical forces are distributed across the hanger brackets and air bags. Longitudinal forces due to braking are applied to the trailer frame through the hanger brackets.

The equilibrium equations of the forces and moments acting on the suspension with unsprung weights G_{21} and G_{22} are expressed as follows:

$$\sum X = z \cdot G_{21} - T_{21} + T_2 - = 0 \quad (53)$$

$$\sum Z = R_{21} - R_2 - R_3 - G_{21} = 0 \quad (54)$$

$$\sum M_3 = -R_3c + R_{21}c_1 - G_{21}c_1 - z \cdot G_{21}(h_s - h_2) + T_{21}h_s = 0 \quad (55)$$

$$\sum X = z \cdot G_{22} - T_{22} + T_4 - = 0 \quad (56)$$

$$\sum Z = R_{22} - R_4 - R_5 - G_{22} = 0 \quad (57)$$

$$\sum M_4 = -R_5c + R_{22}c_1 - G_{22}c_1 - z \cdot G_{22}(h_s - h_2) + T_{22}h_s = 0 \quad (58)$$

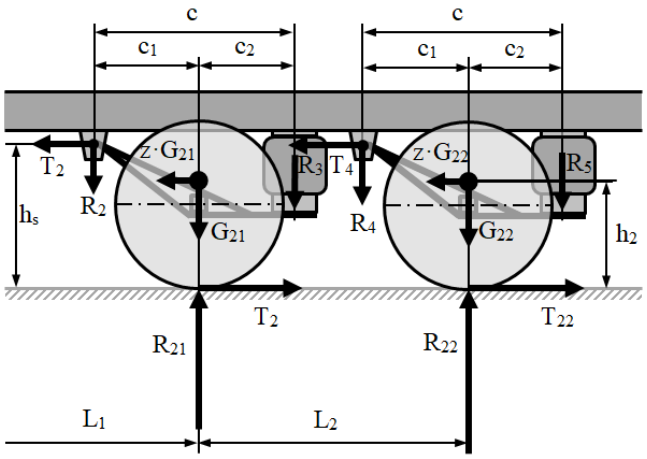

Fig. 7. Forces acting on air tandem suspension

Assuming that the pressure in the airbags is the same, the vertical reactions transmitted by the air springs are equal ($R_3 = R_5$). Then from Eqs. (55) and (58), at ($G_{21} = G_{22}$), the relationship between the tandem axle loads is obtained as:

$$R_{21}c_1 + T_{21}h_s = R_{22}c_1 + T_{22}h_s \quad (59)$$

Solving the system of Eqs. (9), (10) and (59), the trailer axle loads are obtained as:

$$R_1 = G\left(1 - \frac{a}{L} + z\frac{h}{L}\right) + \frac{L_2}{2L}(T_{21} - T_{22})\frac{h_s}{c_1} \quad (60)$$

$$R_{21} = \frac{1}{2}G\left(\frac{a}{L} - z\frac{h}{L}\right) - \frac{L_1 + L_2}{2L}(T_{21} - T_{22})\frac{h_s}{c_1} \quad (61)$$

$$R_{22} = \frac{1}{2}G\left(\frac{a}{L} - z\frac{h}{L}\right) + \frac{L_1}{2L}(T_{21} - T_{22})\frac{h_s}{c_1} \quad (62)$$

where $L = L_1 + L_2/2$.

4. METHOD OF SELECTION OF LINEAR BRAKE FORCE DISTRIBUTION

In compressed air brake systems of agricultural vehicles, different types of load-dependent brake force regulators are used to achieve an approximation of an ideal brake force distribution. The automatic load sensing valves (LSV) currently mounted on heavy trailers have the task of adjusting the braking pressure on an axle (or possibly several axles) relative to the respective load status [32]. With properly designed braking forces, this prevents locking of the wheels when the vehicle is unladen or partially laden. In mechanically suspended trailers, the regulation is relative to the spring deflection. In air-suspended axles, the braking pressure of the pneumatic brake cylinders is dependent on the control pressure of the air springs.

As the pressure distribution characteristic of the load sensing valve is all substantially a straight line, the distribution of braking forces between the front and rear axles can also be considered as linear (radial).

A direction coefficient of the brake force distribution line passing through the origin of coordinate system $T_{2T}=f(T_1)$ is calculated as the braking force ratio:

$$i_P = \frac{T_{21}+T_{22}}{T_1} = \frac{T_{2T}}{T_1} \tag{63}$$

where T_{2T} is the total braking force of the tandem axles.

Similarly, a linear distribution of braking forces, variable or fixed (in the absence of a regulator of braking forces), can be applied to the tandem axle unit as:

$$i_S = \frac{T_{22}}{T_{21}} \tag{64}$$

Using the relations (8), (63) and (64), the braking forces can be described by a parametric equation with the braking rate z as a variable:

$$T_1 = z \cdot G \frac{1}{1+i_P} \quad T_{2T} = z \cdot G \frac{i_P}{1+i_P} \quad T_{21} = T_{2T} \frac{1}{1+i_S}$$
$$T_{22} = T_{2T} \frac{i_S}{1+i_S} \tag{65}$$

The values of the i_P and i_S ratios can theoretically change in a very wide range from zero to infinity; extreme values are achieved if the braking force of one of the axles is equal to zero. Therefore, the braking force distribution coefficients were used to represent the participation of each axle's braking force (braking force distribution proportion), and defined as the ratio of the braking force of the individual axle to the total braking force of the trailer. Namely:

$$\beta_1 = \frac{T_1}{z \cdot G} \quad \beta_2 = \frac{T_{2T}}{z \cdot G} \quad \beta_{21} = \frac{T_{21}}{z \cdot G} \quad \beta_{22} = \frac{T_{22}}{z \cdot G} \tag{66}$$

The values of these coefficients can theoretically change from 0 to 1, and in addition, the following relations are fulfilled:

$$\beta_1 + \beta_2 = 1 \qquad \beta_{21} + \beta_{22} = \beta_2 \tag{67}$$

Using relations (66) and (67), the braking force of a single axle and tandem axle unit can be calculated as:

$$T_1 = \beta_1 z \cdot G \qquad T_{2T} = (1-\beta_1) z \cdot G \qquad T_{21} = \beta_{21} z \cdot G$$
$$T_{22} = (1-\beta_1-\beta_{21}) z \cdot G \tag{68}$$

In order to find the optimal solutions for the linear braking force distribution, the Monte Carlo method [5, 17, 22] was used to search for an acceptable range of variability of the β_1 and β_{21} coefficients. An example block diagram of the algorithm for optimal selection of the braking force distribution coefficients is shown in Fig. 8.

The optimum values of the braking force distribution coefficients are determined in the process of minimizing the objective function consisting of the residual sum of squares:

$$OF = \frac{w_1(f_1-f_2)^2 + w_2(f_{21}-f_{22})^2}{w_1+w_2} \tag{69}$$

where w_i are the weighting factors.

The objective function formulated in this way prefers solutions with the smallest differences between the values of adhesion f_i utilized by individual axles. Since to meet the requirements (3)–(6), it is more important to reduce the difference between adhesion values f_1 of the front axle and f_2 of the rear axle assembly than to reduce the difference between values of adhesion f_{21} and f_{22} utilized by the rear axles, therefore $w_1>w_2$ should be taken in the OF criterion.

Before calculating the objective function, the inequality constraints (3), (4) for the first solution or (5), (6) for the second solution are checked:

$$f_1^{up} \geq f_1 = \frac{T_1}{R_1} \geq f_1^{down} \qquad f_2 = \frac{T_{21}+T_{22}}{R_{21}+R_{22}} \leq f_2^{up} \tag{70}$$

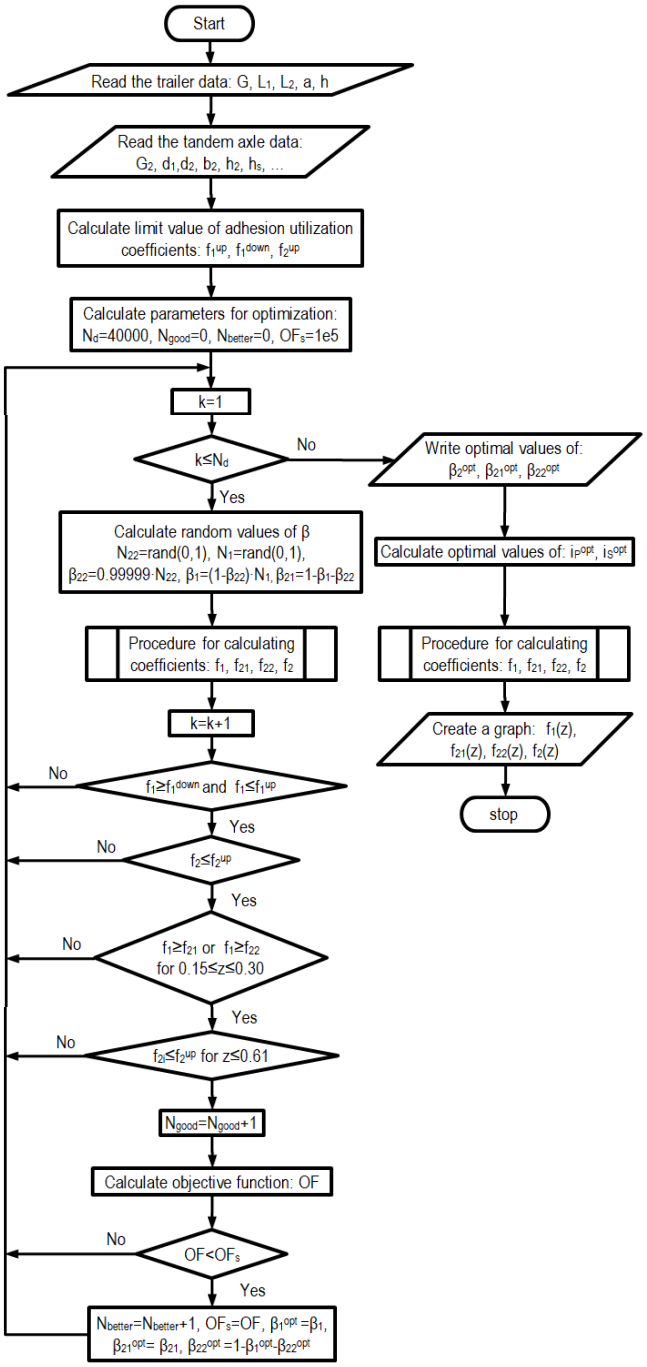

Fig. 8. Block diagram of an algorithm for the optimization of brake forces of a three-axle trailer using the Monte Carlo method (OF_s – initial value of the objective function, N_d – number of draws, N_{good} – number of good solutions, meeting inequality constraints, N_{better} – number of better solutions, reducing the value of the objective function)

In order to simplify the notation of borderline equations, they have been presented as the product of the algebraic and logical expressions. For the first solution:

$$f_1^{down} = z \cdot (0.15 \leq z \leq 0.30) \tag{71}$$

$$f_1^{up} = f_2^{up} = (z+0.07)/0.85 \cdot (0.10 \leq z \leq 0.61) \tag{72}$$

For the second solution:

$$f_1^{down} = (z-0.08) \cdot (0.15 \leq z \leq 0.30) \tag{73}$$

$$f_1^{up} = (z+0.08) \cdot (0.15 \leq z \leq 0.30) \tag{74}$$

DOI 10.2478/ama-2022-0023

$$f_2^{up} = (z + 0.08) \cdot (0.15 \le z \le 0.30) + \left(\frac{z-0.3}{0.7381} + 0.36\right) \cdot (0.3 < z \le 0.61) \quad (75)$$

Then condition (7) for multi-axle vehicles is checked:

$$f_1 > f_{21} \quad \text{or} \quad f_1 > f_{22} \quad \text{for } z = 0.15 \div 0.30 \quad (76)$$

In addition, an extra condition is adopted for the adhesion utilized rates of the rear axle:

$$f_{2i} \le f_2^{up} \quad \text{for } z \le 0.61 \quad (77)$$

which in fact limits excessive increase of the coefficient f_{22} for $z \le 0.61$.

5. RESULTS OF OPTIMIZATION CALCULATIONS

Based on the algorithm described above, a computer program was developed in the MATLAB environment [31] to calculate the optimal distribution of braking forces for three-axle trailers with tandem rear axle suspension. The MATLAB algorithm of the Hammersley sequence [12] from Burkardt [2] was used to generate quasi-random numbers N_{22} and N_1 (Fig. 8). The Hammersley Point Set in two dimensions is one of the simplest low discrepancy sequences and has been used in numerical and graphics applications, with a significant improvement in terms of error [33].

The technical data of the laden and unladen trailer as well as the data of tandem suspensions adopted for optimization calculations are presented in Tab. 2. To ensure comparability of the calculation results, the same mass m_2 = 1,700 kg was used for all types of suspension and some geometrical parameters of suspensions obtained based on the literature data [1, 3] were unified. Changes in some suspension dimensions for laden and unladen weight were also omitted.

The results of calculation of the braking force distribution for the laden and unladen trailer are presented in Tabs. 3 and 4. The number of draws was set as N_d = 40,000. The objective functions (69) were calculated in the range of $0.1 \le z \le 0.66$ with a step size of 0.01 for the following values of weighting factors $w_1 = 0.6$ and $w_2 = 0.4$.

For most types of tandem suspension, the same values of the optimal braking force distribution ratios were obtained (Tab. 3), applying both solutions described in section 2. The values after the dash are obtained taking into account the weight of the tandem suspension.

Tab. 2. Trailer and tandem suspension technical data [1, 3]

Trailer		Tandem suspension				
Unladen	**Laden**	**Bogie (3.1)**	**Two leaf spring (3.2)**	**Two leaf two rod (3.3)**	**Two leaf equal. (3.4)**	**Air susp. (3.5)**
m = 7,700 kg	m = 24,000 kg	d_1 = 0.705 m	c_1 = 0.454 m	c_1 = 0.497 m	c_1 = 0.454 m	c_1 = 0.5 m
L_1 = 4.35 m	L_1 = 4.35 m	d_2 = 0.645 m	c = 0.93 m	c = 0.97 m	c = 0.93 m	c = 0.88 m
L_2 = 1.35 m	L_2 = 1.35 m	h_s = 0.567 m	h_s = 0.717 m	$h_{r1} = h_{r1}$ = 0.467 m	h_s = 0.717 m	h_s = 0.717 m
a = 3.11 m	a = 3.04 m	h_2 = 0.547 m	h_2 = 0.567 m	h_2 = 0.567 m	h_2 = 0.567 m	h_2 = 0.567 m
h = 1.19 m	h = 1.57 m	b_2 = 0.03 m	$d_1 = d_2$ = 0.21 m	$d_1 = d_2$ = 0.19 m	$d_1 = d_2$ = 0.675 m	
				$\alpha_1 = \alpha_2$=15°		

Tab. 3. The results of the optimization of brake force distribution in a three-axle trailer for suspension described in sections 3.1 and 3.3–3.5 (L – laden, U – unladen, L_w, U_w – laden and unladen with weight of suspension)

Suspension		OF	β_1	β_{21}	β_{22}	i_P	i_S
Bogie (3.1)	U-U_w	0.2051–0.2049	0.4755–0.4758	0.3563–0.3608	0.1682–0.1634	1.1031–1.1018	0.4722–0.4530
	L-L_w	0.2638–0.2631	0.5359–0.5298	0.3167–0.3264	0.1473–0.1438	0.8659–0.8876	0.4651–0.4406
2 leaf 2 rod (3.3)	U-U_w	0.2831–0.3681	0.5311–0.5364	0.1316–0.1162	0.3373–0.3475	0.8827–0.8645	2.5632–2.9910
	L-L_w	0.3708–0.3989	0.5888–0.5849	0.1141–0.1085	0.2971–0.3067	0.6982–0.7098	2.6041–2.8276
2 leaf equal. (3.4)	U-U_w	0.0585–0.0707	0.4881–0.4983	0.2553–0.2548	0.2565–0.2469	1.0486–1.0068	1.0046–0.9692
	L-L_w	0.1016–0.1082	0.5413–0.5413	0.2296–0.2296	0.2291–0.2291	0.8473–0.8473	0.9981–0.9981
air susp. (3.5)	U-U_w	0.0585–0,0585	0.4881–0,4881	0.2553–0.2553	0.2565–0.2565	1.0486–1.0486	1.0046–1.0046
	L-L_w	0.1016–0.1016	0.5413–0.5413	0.2296–0.2296	0.2291–0.2291	0.8473–0.8473	0.9981–0.9981

Tab. 4. The results of the optimization of brake force distribution in a three-axle trailer for two leaf spring suspension described in section 3.2 (L-laden, U-unladen, L_w, U_w – laden and unladen with weight of suspension)

Solution		OF	β_1	β_{21}	β_{22}	i_P	i_S
I	U-U_w	1.3757–1.0286	0.6269–0.5973	0.0573–0.0641	0.3158–0.3386	0.5952–0.6743	5.5072–5.2780
	L-L_w	1.4814–1.3513	0.6734–0.6542	0.0484–0.0452	0.2782–0.3006	0.4850–0.5285	5.7452–6.6487
II	U-U_w	1.5155–1.0286	0.6009–0.5973	0.0371–0.0641	0.3620–0.3386	0.6641–0.6743	9.7537–5.2780
	L-L_w	1.7692–1.4772	0.6426–0.6417	0.0267–0.0363	0.3308–0.3220	0.5563–0.5583	12.401–8.8715

Slightly different values of the optimal coefficients of the braking force distribution for the first and second solutions were obtained for the two leaf spring suspension (section 3.2) and therefore they are presented separately in Tab. 4.

Based on the calculation results of the β_1, β_{21}, β_{21}, i_P and i_S ratios presented in Tabs. 3 and 4, it can be seen that the distribution of the braking forces in a three-axle trailer significantly depends on the trailer loading and tandem suspension used in it.

The air suspension (section 3.5) and two leaf spring suspension with equalization (section 3.4) can be considered as the best in terms of the optimization criterion used (lowest OF value).

The trailer with these suspensions has a uniform distribution of braking forces, close to the ideal one, at which the value of coefficient β_1 is about 50%, the values of coefficients β_{21} and β_{22} are about 25%, and values of the i_P and i_S coefficients are about 1. Greater values of the objective function OF were obtained for the bogie suspension (section 3.1) and even greater for the two leaf–two rod suspension (section 3.3). Nevertheless, for all these suspensions, the same values of calculated parameters of the braking force distribution were obtained, regardless of the applied solution. However, this does not apply to the suspension (3.2), which, due to the calculated values of the objective function, differs significantly from the others.

The results of calculating the brake force distribution coefficients for two leaf spring suspension indicate a large variation in the distribution of the braking forces of tandem axles, where the β_{21} coefficient of the leading axle is only about 2.7–6.4%. This may cause wheel lock on this axle according to the literature [13, 18]. An example of the course of the adhesion utilization rates $f_i(z)$ through the axles for an optimal distribution of brake forces for an unladen and a laden trailer with two leaf spring tandem suspension is shown in Fig. 9a and c. The adhesion utilization curve f_{21} of the leading tandem axle tends to infinity for $z > 0.7$ in the case of the unladen trailer (Fig. 9a) and for $z > 0.65$ in the case of the laden trailer (Fig. 9c) due to wheel separation from the road surface ($R_{21} = 0$). Meanwhile, for a trailer with air suspension of tandem axles, the adhesion utilization curves f_{21}, f_{22} and f_2 almost match for both the unladen (Fig. 9b) and laden trailers (Fig. 9d), which means that the coefficients of the adhesion utilization of both tandem axles are the same.

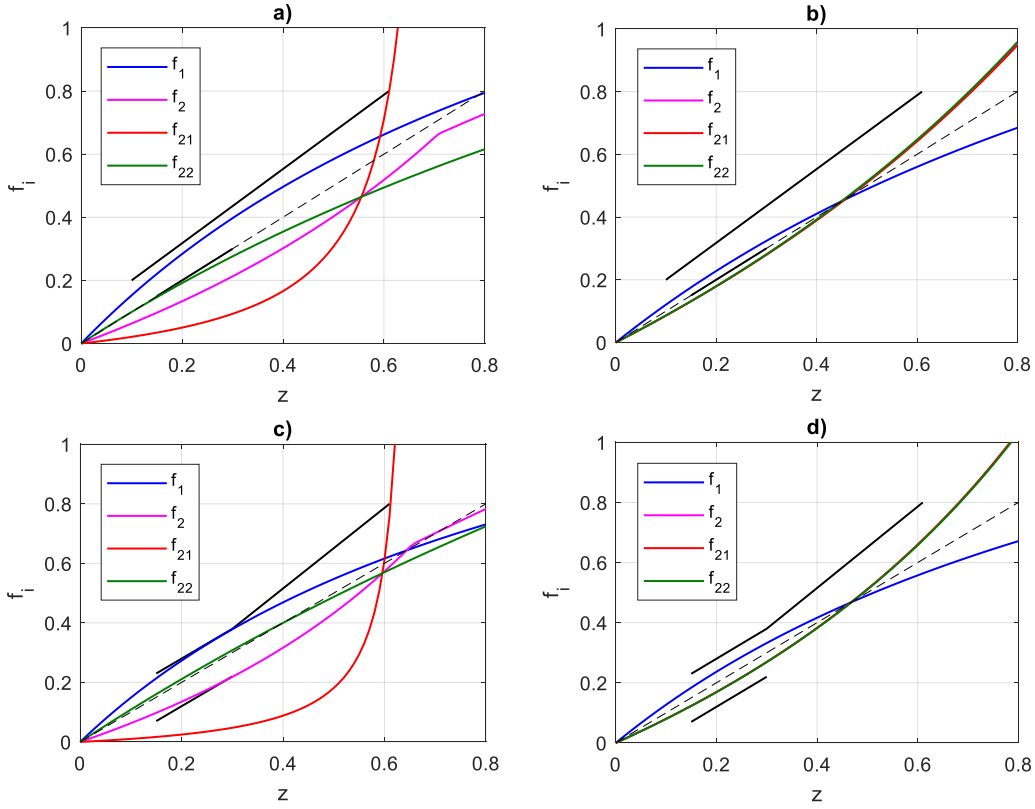

Fig. 9. The runs *fi(z)* for an optimal distribution of brake forces in a three- axle trailer (disregarding the weight of the tandem suspension): (a) – an unladen trailer with two leaf spring tandem suspension (I solution), $\beta_{21} = 5.7\%$, $\beta_{22} = 31.6\%$; (c) – a laden trailer with two spring tandem suspension (II solution), $\beta_{21} = 2.7\%$, $\beta_{22} = 33.1\%$; (b) – an unladen trailer with air tandem suspension, $\beta_{21} = 22.5\%$, $\beta_{22} = 25.6\%$; (d) – a laden trailer with air tandem suspension (II solution), $\beta_{21} = 23\%$, $\beta_{22} = 22.9\%$

Comparing the calculation results obtained without and with the weight of the tandem suspension, it can be concluded that, in the case of suspensions 3.1, 3.4 and 3.5, the influence of this weight on the distribution of braking forces is negligible. The differences in the values of the braking force distribution coefficients do not exceed 1%. However, in the case of suspension 3.3, the differences in the calculated values of the is coefficient amount to approximately 16.7%, and in the case of suspension 3.2, even up to 46%.

6. SUMMARY AND CONCLUSIONS

The described method of optimizing the selection of the linear distribution of the braking forces of heavy three-axle agricultural trailers with various types of rear tandem axles can be used in the design of air braking systems, in which braking force correctors with radial characteristics were applied. The calculations of the braking force distribution took into account the requirements of the

EU Directive 2015/68 [6] in terms of braking performance and stability.

Optimization calculations made with the Monte Carlo method for a three-axle trailer with a load capacity of about 16 tonnes showed that the distribution of the braking forces significantly depends on the type of tandem suspension of the rear axles. The lowest values of the minimized objective function were achieved with the use of tandem axles with air suspension and two leaf spring suspension with equalization. For these two tandem suspensions, the adhesion utilization rates for individual axles are closest to the straight line illustrating the ideal distribution of braking forces, in which the adhesion utilized by each axle is the same and equal to the braking rate. The values for the β2i ratios of the individual tandem axle and the total braking force of trailer are equalised and range from approximately 22.9% to 25.5% for the various calculation variants (I and II solution, laden and unladen trailer, without and with unsprung weight). The highest values of the objective function were obtained for the two leaf spring tandem suspension. For this suspension, the β21 ratio of the leading axle ranges from 2.7% to 6.4% and the β22 ratio of the trailing axle from 27.8% to 36.2%. Moreover, the calculations showed that the load transfer between the axles of this tandem suspension can lead to premature blocking of the leading axle wheels at braking ratios above 0.65. The results of the calculations are qualitatively consistent with the findings presented in [13, 18].

From the optimization calculation results obtained without and with the weight of the tandem suspension, it can be concluded that in the case of suspensions 3.1, 3.4 and 3.5, the influence of this weight on the distribution of braking forces is negligible.

REFERENCES

1. Agriculture Equipment Brochure. 2015. Available from: http://www.bpwtranspec.com.au/wp-content/uploads/2013/03/BPW_Agriculture_Equipment_brochure.pdf
2. Burkardt J. The Hammersley Quasi Monte Carlo (QMC) Sequence. Available from: https://people.sc.fsu.edu/~jburkardt/m_src/hammersley/hammersley.html
3. Colaert Essieux. General Catalogue. 2019. Available from: http://www.colaertessieux.fr/PDF/COLAERT-ESSIEUX-GENERAL-CATALOGUE.pdf
4. Day A.J. Braking of Road Vehicles. Oxford: Butterworth-Heinemann, 2014.
5. Dimov IT. Monte Carlo Methods for Applied Scientists. World Scientific; 2007. Available from: https://www.worldscientific.com/worldscibooks/10.1142/2813
6. European Commission. Commission Delegated Regulation (EU) 2015/68 of 15 October 2014 supplementing Regulation (EU) No 167/2013 of the European Parliament and of the Council with regard to vehicle braking requirements for the approval of agricultural and forestry vehicles. 2015.
7. Fancher P, Winkler C. Directional performance issues in evaluation and design of articulated heavy vehicles. Vehicle System Dynamics. 2007;45(7–8):607–47.
8. Gillmann R. Axle spacing and load equivalency factors. Transportation Research Record: Journal of the Transportation Research Board. 1999;1655(1):227–32.
9. Glišović J, Lukić J, Šušteršič V, Ćatić D. Development of tractors and trailers in accordance with the requirements of legal regulations. In: 9th International Quality Conference. Faculty of Engineering, University of Kragujevac; 2015; 193–202.
10. Goodarzi A, Behmadi M, Esmailzadeh E. An optimised braking force distribution strategy for articulated vehicles. Vehicle System Dynamics. 2008;46(sup1):849–56.
11. Ha, DV, Tan, VV., Niem, VT., Sename, O. Evaluation of Dynamic Load Reduction for a Tractor Semi-Trailer Using the Air Suspension System at all Axles of the Semi-Trailer. Actuators 2022;11:12. https://doi.org/10.3390/act11010012
12. Hammersley JM. Monte Carlo methods for solving multivariable problems. Numerical Properties of Functions of Moe Than One Independent Variable. 1960;86(3):844–74.
13. Harwood DW. Review of Truck Characteristics as Factors in Roadway Design. Washington, D.C.: Transportation Research Board; 2003. Available from: https://www.nap.edu/catalog/23379
14. Heisler H. 10 - Suspension. In: Heisler H, editor. Advanced Vehicle Technology. 2nd ed. Oxford: Butterworth-Heinemann; 2002; 368–449.
15. ISO 8855:2011. Road vehicles — Vehicle dynamics and road-holding.
16. Kamiński Z, Radzajewski P. Calculations of the optimal distribution of brake force in agricultural vehicles categories R3 and R4. Eksploat i Niezawodn. 2019;21(4):645–53.
17. Kroese DP, Taimre T, Botev ZI. Handbook of Monte Carlo Methods. Wiley; 2011.
18. Limpert R. Engineering Design Handbook: Analysis and Design of Automotive Brake Systems. HQ, US Army Materiel Development and Readiness Command; 1976.
19. Limpert R. An investigation of the brake force distribution on tractor-semitrailer combinations. Society of Automotive Engineers; 1971. Available from: https://www.sae.org/content/710044/
20. Miatluk M, Kaminski Z. Brake systems of road vehicles. Calculations. Bialystok: Wydawnictwo Politechniki Bialostockiej; 2005.
21. Mital A, Desai A, Subramanian A, Mital A. Product development: A structured approach to consumer product development, design, and manufacture. 2nd ed. Elsevier Science; 2014.
22. Morton DP, Popova E. Monte-Carlo Simulations for Stochastic Optimization. In: Encyclopedia of Optimization. Boston, MA: Springer US; 1529–37.
23. NHTSA heavy duty vehicle brake research program: Report no. 1 – stopping capability of air braked vehicles. National Highway Traffic Safety Administration; 1985. by Richard W. Radlinski and S. F. Williams. Available from: https://books.google.pl/books?id=pfbZvgEACAAJ
24. Nunney MJ. Light and Heavy Vehicle Technology. Routledge; 2007.
25. Pierce PR. Controlled load transfer during braking on a four-spring trailer suspension. Society of Automotive Engineers; 1985. Available from: https://www.sae.org/content/852344/
26. [26] Road Safety Authority. Revised Standards for Agricultural Vehicles RSA Guide. Ballina, Republic of Ireland: Road Safety Authority; 2015.
27. Sun B, Wang P, Gao S, Yu J, Wang Z. Development of braking force distribution strategy for Dual-Motor-Drive Electric Vehicle. Journal of Engineering and Technological Sciences. 2018;50(2):179–201.
28. Tang G, Zhao H, Wu J, Zhang Y. Optimization of braking force distribution for three-axle truck. Society of Automotive Engineers; 2013. Available from: https://www.sae.org/content/2013-01-0414/
29. Titan Agricultural Catalogue – Tires, wheels, tracks, axles. 2015. Available from: http://titanaust.com.au/wp-content/uploads/2015/10/TITA0053-C1L3P2-Agricultural-Catalogue-COMPLETE_LR.pdf
30. Van Straelen B. Lastverlagerung und Bremskraftverteilung bei Einachs- und Doppelachsanhängern. Grundlagen der Landtechnik. 1983;33(6):183–9.
31. Venkataraman P. Applied Optimization with MATLAB Programming. 2nd ed. Hoboken: Wiley & Sons, Inc.; 2009
32. WABCO. Pneumatic Braking System Agriculture and Forestry. Product Catalogue. 2017. Available from: https://www.wabco-customercentre.com/catalog/docs/8150100823.pdf

33. Wong T-T, Luk W-S, Heng P-A. Sampling with Hammersley and Halton Points. Journal of Graphics Tools. 1997;2(2):9–24.
34. Xu J, Zhang X. Optimization algorithm for vehicle braking force distribution of front and rear axles based on brake strength. 12th World Congress on Intelligent Control and Automation (WCICA). IEEE; 2016; 3353–60.
35. Zhao LH, Cao QG, Li YS, Gao NZ. An optimization technique of braking force distribution coefficient for truck. Proceedings 2011 International Conference on Transportation, Mechanical, and Electrical Engineering (TMEE). IEEE. 2011;1784–7.

NOMENCLATURE

i – tandem axle index (i=1, leading axle; i=2 , trailing axle)
a – distance from the centre of gravity to front axle [m]
b_2 – distance of centre of unsprung weight from a support [m]
c – leaf spring length [m]
c_1 , c_2 – leaf spring arm length [m]
c_{ri} – i-th distance from rod pivot to centre of axle [m]
d_1 , d_2 – beam (parabolic spring) length, equalizer beam length [m]
f_1, f_2 – adhesion utilization rate of front and rear axle assembly
G – trailer weight [N]
G_2 – unsprung weight of beam (parabolic spring) [N]
G_{2i} –unsprung weight of i-th tandem axle [N]
h – centre of gravity height [m]
h_s – height of support position [m]
h_2 – height of centre of unsprung weight [m]
h_{ri} – i-th rod pivot height [m]
i_P – braking force ratio
i_S – tandem braking force ratio
L_1 – inter-axle spacing [m]
L_2 – tandem axle spread [m]
R_1 – front axle load [N]
R_{2i} – i-th tandem axle load [N]
T_1 – front axle braking force [N]
T_{2i} – i-th braking force of tandem axle [N]
z – braking rate of trailer [-]
α_i – i-th rod angle [º]
β_1 – ratio of front axle to total braking force
β_2 – ratio of tandem axle to total braking force
β_{2i} – ratio of i-th tandem axle to total braking force

Acknowledgments: This research was founded through subsidy of the Ministry of Science and Higher Education of Poland for the discipline of mechanical engineering at the Faculty of Mechanical Engineering Bialystok University of Technology WZ/WM-IIM/4/2020.

Zbigniew Kamiński: https://orcid.org/0000-0003-2693-5077